J Mater Sci: Mater Med (2008) 19:3135–3144
DOI 10.1007/s10856-008-3434-1

Towards a controlled photopolymerization of dental dimethacrylate monomers: EPR studies on effects of dilution, filler loading, storage and aging

S. G. Pereira · J. P. Telo · T. G. Nunes

Received: 8 November 2007 / Accepted: 11 March 2008 / Published online: 15 April 2008

Abstract Electron paramagnetic resonance (EPR) was used to study the kinetics of methacrylate radical formation in the monomer mixture 2,2-bis [4-(2-hydroxy-3-methacryloxyprop-1-oxy) phenyl] propane (Bis-GMA)/triethylene glycol dimethacrylate (TEGDMA), in the presence of a photo-initiator system (camphorquinone, CQ/*N*,*N*-dimethyl-*p*-toluidine, DET). Curing-time dependences on the filler (0–40 wt%) and TEGDMA content (15–90 wt%) were evaluated; the influence of irradiation protocol, uncured sample storage time and aging of cured systems were also studied. EPR enabled observing at least two different kinetic regimes during polymerization. The final radical concentration decreased both with Bis-GMA and filler content. However, a reverse trend was obtained when the relative photo-initiator concentrations were considered. Filler also showed a significant effect on the radical life--time reduction. Irradiation protocol and storage time of uncured matrices showed to affect the free radical concentration. The observed changes on the EPR signal lineshape with post-curing time suggests that the distribution of CH_2 conformations also changes with time.

S. G. Pereira (✉) · T. G. Nunes
Materials Engineer Department and CQE, IST,
Technical University of Lisbon, Av. Rovisco Pais, 1,
Lisboa 1049-001, Portugal
e-mail: soniag.pereira@ist.utl.pt

J. P. Telo
Chemistry and Biological Department and CQE, IST,
Technical University of Lisbon, Av. Rovisco Pais, 1,
Lisboa 1049-001, Portugal

1 Introduction

Dental restorative composite materials are generally light-cured by radical polymerization of methacrylate monomers, which proceeds via adding monomers to the growing polymer chains. A particulate filler is always present, at different loads, in order to improve the final mechanical performance.

The camphorquinone (photosensitive-initiator)/amine (co-initiator reducing agent) system is widely used in the first reaction stage of polymerization of dental materials [1–3]. Amine radicals add to the double bonds of methacrylate groups and generate new radicals that further react successively with monomers to form a cross-linked network; the propagation reaction then leads to the increase of the matrix viscosity. This reaction occurs until no additional monomer is able to react or the propagation reaction is stopped by termination.

It is recognized that these radicals achieve sufficient concentrations to be observed by EPR in the latter periods of a four-stage polymerization process: stages I–III that origin the auto-acceleration period (gelation), during which polymeric and segmental chains can move by translational diffusion, and stage IV, i.e. auto-deceleration period (vitrification), during which only segmental diffusion and macromolecular conformational transitions are possible [4, 5]. A more detailed description of these four stages is given in Sect. 3. The reduced mobility of the polymer network, formed during vitrification, leads to incomplete double bond conversion of unreacted dimethacrylate monomers and pendant methacrylate groups. In fact, the network of a light-cured composite, with a glass-transition temperature higher than the reaction temperature, includes remaining double bonds and molecules with one or two free radicals which are located at functional groups. These radicals,

which have been extensively studied by EPR and ENDOR spectroscopy over the last 50 years, are very reactive, and their concentration decays logarithmically with time [6]. At a constant storage temperature, the half-life of radicals depends on the type of filler, the filler fraction, the filler surface treatment and viscosity. However, the role of these parameters on the final restorative dental materials properties is not completely understood [7, 8].

EPR is a powerful tool to detect radicals present in these photo-cured systems, enabling the study of structure, concentration and half-life of the radicals formed. Monitoring these parameters provides insight into the mechanism of polymerization, the nature of the polymerization kinetics, and the network durability [9].

The incomplete conversion of double bonds commonly achieved in photo-cured dental polymers (<85%) affects the material performance in vivo and may induce toxicity problems due to the leaching-out of unreacted monomers. Aiming to contribute for the improvement of dental materials, we report here the effect of different experimental conditions on the free propagating radical concentration.

2 Materials and methods

2.1 Materials

Three homogeneous co-monomer mixtures of Bis-GMA (Polysciences Inc.) and 15, 50 or 90 wt% TEGDMA (Aldrich Chemical Co., Milwaukee, WI, USA) were prepared with CQ (1 mol%, Aldrich Chemical Co.) and DET (1 mol%, Aldrich Chemical Co.); the photo-initiator system (CQ and DET) was used as received. The chemical structures of Bis-GMA and TEGDMA are shown in Fig. 1.

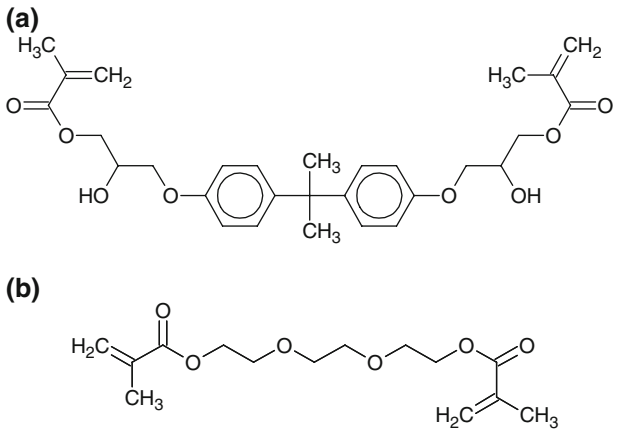

Fig. 1 Structure of: (**a**) 2,2-bis [4-(2-hydroxy-3-methacryloxyprop-1-oxy) phenyl] propane (Bis-GMA); (**b**) triethylene glycol dimethacrylate (TEGDMA)

A homogeneous co-monomer mixture of 75 wt% Bis-GMA and 25 wt% TEGDMA containing the same photo-initiator system, was also prepared and subsequently used to obtain five composite resins with 10, 20, 30 and 40 wt% filler loading; the viscosity of the unfilled resin was about 2 Pa s [6]. The filler was a silanated hybrid filler (Herculite, Kerr, USA) with an average particle size of less than 1 μm. The filler particles were from Ba aluminosilicate glasses and pyrogenic silica treated with the organic silane γ-methacryloxy(propyl)trimethoxysilane.

2.2 Methods

A Bruker ESP 300E spectrometer was used to obtain the EPR spectra. The resins and composite resins were placed in quartz tubes (3 mm inner diameter, 170 mm height) filled up to about 20 mm height; the samples were irradiated outside the spectrometer using a light source (Optilux 401, Demetron Research Corp., Danbury, CT, USA) with light emission between 400 nm and 500 nm, maximum at 470 nm, and 500 mW/cm^2 light intensity. Samples were irradiated from the side of the tubes; during curing, the light tip was moved around the sample tube, in overlapping positions, in order to achieve the maximum conversion degree. The measurements were carried out at 295 K, in air. EPR spectra were acquired prior irradiation and after the following cumulative irradiation periods: (a) 1, 2, 4, 6, 10, 15, 20, 40, 60, 100, 160, 180 s; (b) 1, 2, 4, 10, 15, 20, 30, 60, 100, 140, 200, 300 s and (c) 60, 180, 300 s. Spectral peak to peak heights were used to monitor the variation of free radical concentration with different parameters (irradiation time and protocol, filler and diluent content and aging of the uncured matrices), while keeping constant the volume sample.

To study the storage time effect on polymerization of unfilled and 20 wt% filler loaded resins, EPR spectra were acquired immediately after the sample preparation and after storing the sample over 10 days at 0°C in the dark.

The concentration of free radicals in two Bis-GMA/TEGDMA matrices (0 and 30 wt% filler loaded), also used to evaluate the filler concentration effect, was monitorized over 65 days (samples were not stored in the dark).

3 Results and discussion

The copolymerization of different Bis-GMA/TEGDMA matrices was followed up by EPR. Figure 2 shows typical spectra which were recorded after cumulative irradiation periods up to a total of 300 s was reached. A typical EPR spectrum is composed of nine lines which are assigned to methyl methacrylate radicals; it is difficult to observe amine-primary radicals because their life-times are

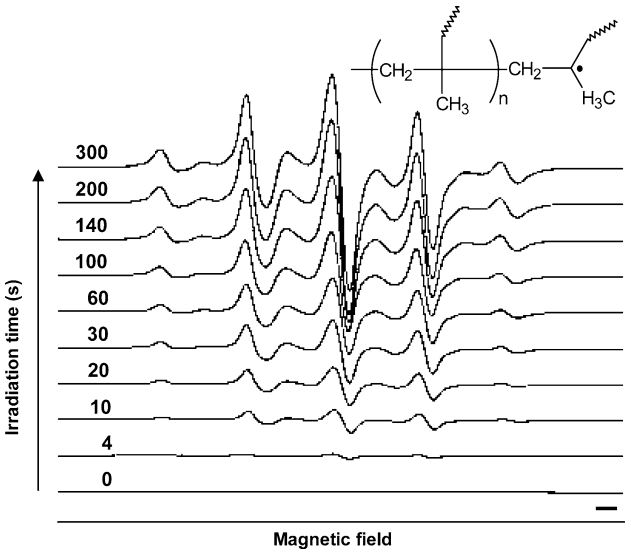

Fig. 2 Typical EPR spectra of methacrylate dental resins obtained during photopolymerization

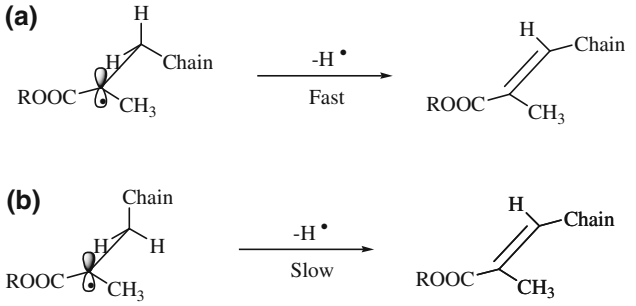

Fig. 4 Oxidation of radicals in different conformations. The elimination is favored by conformations where the H atom bond is parallel to the single-occupied p-orbital (**a**). The reaction is much slower in the most stable conformation (**b**), where the C–H bond is not parallel to the p-orbital bearing the unpaired electron

extremely short. These nine line spectra are generally called 5 + 4 line spectra because of the different intensity ratios between a set of five peaks and another one of four peaks. Such spectra, are generally assigned to a single chemical species (Figs. 3 and 4), with the 5 β protons of the CH_3 (methyl) and CH_2 (methylene) groups being responsible for the hyperfine pattern. The methyl group is rotating freely even at low temperatures, but the conformation of the methylene protons is rigidly fixed due to restricted movement of the polymer chain [10]. However, the experimental spectrum seems to contain a weighted sum of sub-spectra corresponding most possibly to different conformations. Simulations of the ENDOR spectra [10] suggest that the major contribution is from the conformation where the polymer chain makes an angle approximately between 0° and 10° with the p-orbital bearing the unpaired electron (structure B in Fig. 4). This orientation corresponds to the most stable conformation, because it maximizes the distance between bulky substituents. Some researchers have suggested that the nine-line spectrum (Fig. 2) is due to two different radical species: the propagating radical obtained by addition to the methacrylate double bond and an allylic radical produced by hydrogen abstraction from the CH_3 group [2, 6]. However, the experimental spectra can be simulated by considering only one radical [10], and the secondary allylic radical is not likely to be produced in amounts sufficient to significantly affect the EPR spectra. Therefore, we admit the simplest scenario, that the EPR spectra is due to only one radical.

The results (Figs. 5 and 6) interpretation is supported by the hypothesis that we are in the presence of a four-stage reaction, as already mentioned in Introduction (Sect. 1). When low or no extent of polymerization has taken place, the viscosity of the reacting system remains low; hence, the mobility of the propagating free radicals favors the termination process by a bimolecular reaction (either by dimerization or disproportionation) and/or by reaction with dissolved molecular oxygen (a recognized free radical scavenger [2]). Typically, these termination processes keep the propagating free radical concentrations low and undetectable. (II) In a first intermediate stage, the rapid increase of the radical population from the onset of polymerization is accompanied by an auto-acceleration reaction; because the viscosity increases, mobility decreases and the termination reaction yield decreases, hence the free radicals become EPR detectable. (III) Once the termination drops to low rates, the reaction becomes diffusion controlled. This mechanism is related with the low mobility of the growing chain-end radicals and the termination essentially occurs when an unpaired electron propagates through monomeric

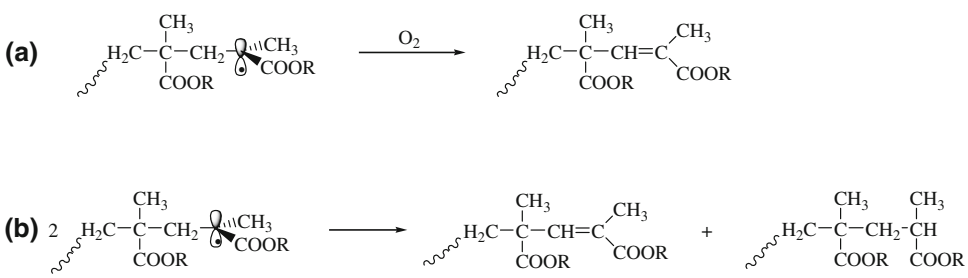

Fig. 3 Pathways for termination reaction of polymer radicals: (**a**) oxidation by molecular oxygen; (**b**) dismutation

(or pendant) double bonds until it reacts with another radical. (IV) A final stage is observed in which additional increase in radical concentration occurs with slow rates. This fact takes place because polymerization has become extensive and initiation, propagation and termination are all diffusion controlled. Even after the sample entered the vitrification period it is possible to detect an increase in methacrylate radical concentration, which is explained by a release of a sufficient number of radicals by photocleavage of the photo-initiator.

3.1 Dilution effect

Experiments were carried out using dimethacrylate monomers commonly present in dental restorative formulation, consisting of a high viscous monomer, Bis-GMA (1,200 Pa s), mixed with different weight ratios of a diluent, TEGDMA (15–90 wt%). The variation of radical concentration with irradiation time, up to 180 s, is shown in Fig. 5a. Three parameter sigmoidal (logistic) functions were used to fit these data:

$$[R^{\bullet}](t) = \frac{[R^{\bullet}]_f - [R^{\bullet}]_i}{1 + \left(\frac{t}{t_h}\right)^p} + [R^{\bullet}]_i, \quad (1)$$

where $[R^{\bullet}]_f$ represents the radical concentration at the end of the reaction (upper asymptote), t_h the time at which half of $R^{\bullet}$ was formed [i.e. t for $([R^{\bullet}]_f)/2$] and $[R^{\bullet}]_i$, the initial free radical concentration, is null. The exponent p is an empirical constant reflecting the trend (positive for growth) and asymmetry shown by the $[R^{\bullet}](t)$ curve around its inflection point, which can be correlated to free radical termination constraints by diffusion. Pintar et al. have expressed the variation of radical concentration with irradiation time, taken into account the depth of cure, by means of a two fitting parameter exponential equation [11]. However, in the present study, the use of Eq. 1 provided a higher correlation factor. Figure 5a shows the sigmoidal fitting curves generated using the parameters indicated in Table 1. Two different regimes were observed during the irradiation period: (a) the concentration of free radicals was higher for lower diluted matrices over the first 4 s and (b)

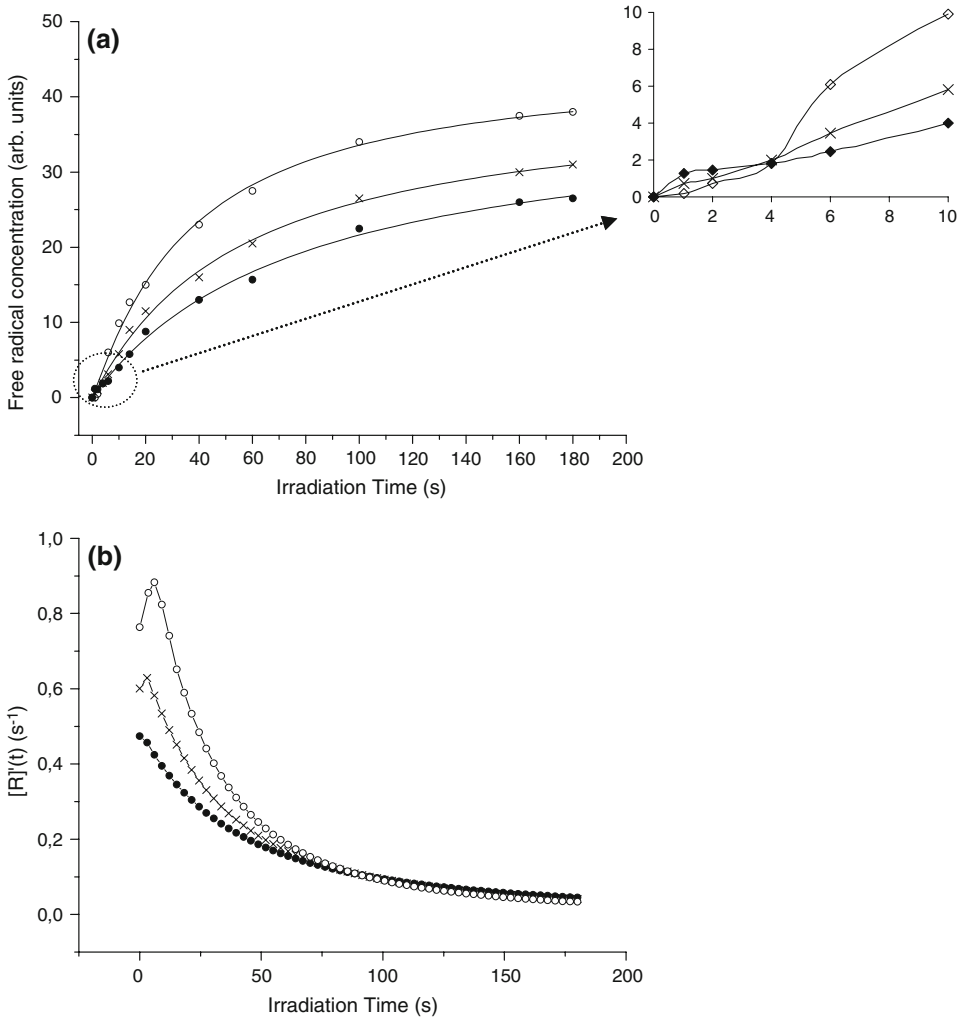

Fig. 5 Free radical concentration variation with irradiation time obtained over 300 s for Bis-GMA resins with different TEGDMA content: (○) 90 wt% diluent, (×) 50 wt% TEGDMA and (•) 90 wt% TEGDMA

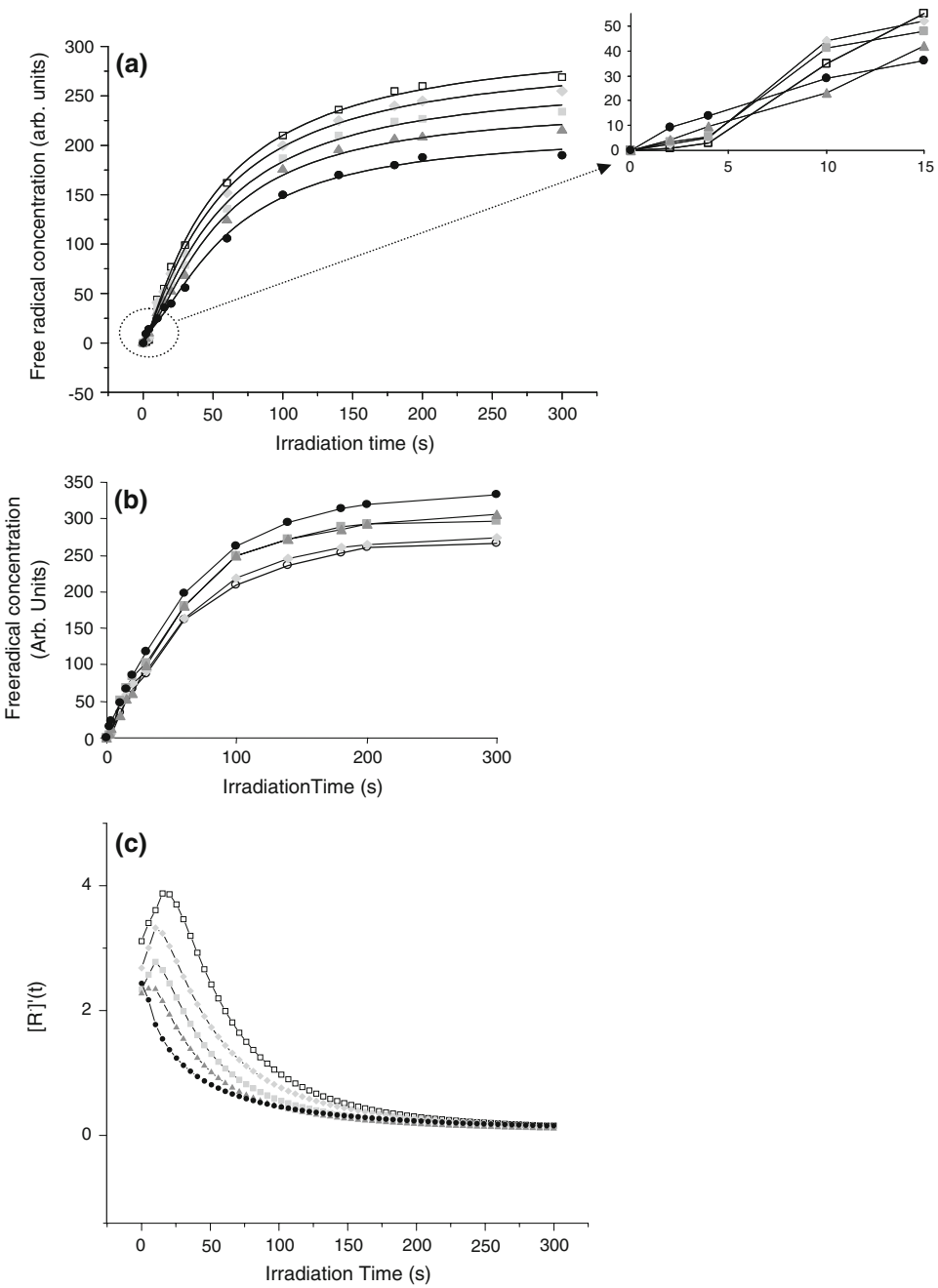

Fig. 6 Data obtained for Bis-GMA/TEGDMA (75/25) matrices with different filler content, which were irradiated over 300 s (○, 0 wt% filler, ♦, 10 wt% filler, ■, 20 wt% filler, ▲, 30 wt% filler and •, 40 wt% filler): (**a**) free radical concentration variation with irradiation time and sigmoidal fitting curve (Eq. 1); (**b**) reaction rates determined using Eq. 2 and (**c**) free radical concentration variation with irradiation time, which were obtained for each sample by multiplying EPR data by the relative concentration of the photo-initiator; the lines are just eye guides

an opposite trend was observed from about 4 to 180 s. These results may be explained on the basis of the viscosity influence on the four-stage reaction mechanism (I–IV), which was previously mentioned [5]. In regime (a), the starting monomeric system viscosity appears to control the radical termination kinetics; hence, a less viscous system like (Bis-GMA/90 wt% TEGDMA) favours the radical termination reaction and, accordingly, the presence of free radicals remain low or undetectable. The polymerization mechanism present in stages I and II (two radicals diffusing, meeting, and reacting by termination) may explain the free radical concentration decrease with the diluent content in this initial regime. Hence, the polymerization period occurring under regime (a) is assigned to stages I and II [5]. In regime (b), the initial viscosity of the reacting matrix did not seem to affect the radical concentration since a rigid network was already formed and consequently the radical termination was reaction controlled or even inhibited; the polymerization period occurring under regime (b) is assigned here to stages III and IV, corresponding to the last step of gelation and to vitrification [5].

The present results also show that the final number of trapped radicals increases with dilution (higher TEGDMA concentration).

Table 1 Parameters of the sigmoidal (logistic) function (Eq. 1) used to fit the variation of radical concentration with irradiation time for Bis-GMA matrix with different TEGDMA content: correlation factor (χ^2, final reached radical content $[R^\bullet]_f$, time t_h to reach $[R^\bullet]_f/2$ and the empirical constant p

TEGDMA (wt%)	90	50	15
χ^2	0.996	0.997	0.997
$[R^\bullet]_f$	44.66 ± 2.27	40.14 ± 2.46	38.50 ± 3.60
t_h	36.41 ± 4.66	54.93 ± 8.19	78.14 ± 16.79
p	1.09 ± 0.08	1.02 ± 0.07	0.99 ± 0.07
$t_{max\ (s)}$	6.10	3.05	–[a]

The time t_{max} to reach the maximum reaction rate is also indicated

[a] Not detectable in the EPR time scale

The polymerization rates were obtained from numerical differentiations (Eq. 2) of the functions used to fit the variation of radical concentration with irradiation time (Eq. 1):

$$[R^\bullet]'(t) = \frac{\left([R^\bullet]_f - [R^\bullet]_i\right) p t^{(p-1)-p}}{(1 + t^p t_h^{-p})^2 [R^\bullet]_f} \quad (2)$$

Overall, despite similar reaction rates being expected, which are mainly determined by using a constant initiator concentration and light intensity, differences were observed that must be explained by different sample reactivities during the polymerizations. Figure 5b presents the polymerization rate ($[R^\bullet]'$) as a function of irradiation time at various diluent (TEGDMA) concentrations; clear differences can be observed for gelation (stages I–III) and vitrification (stage IV) periods as a function of dilution showing an evident role of viscosity on the reaction rate control. For p values between 0 and 1, there is no inflection point in the curve, only a rate decrease corresponding to the vitrification stage. This behaviour is shown by matrices with lower TEGDMA concentration (15 wt%); in this case, gelation has occurred too fast to be observed by EPR. With the increase of diluent concentration, p value also increases and the inflection point is introduced ($P > 1$) in agreement with a less pronounced effect of diffusion constraints in the reaction.

The second derivative of Eq. 1 in order to time t_h is related to the inflection point of the sigmoidal curve, corresponding to the maximum rate of radical production (r_{max}). Data related with the inflection points (t_{max}/s) between auto-acceleration and auto-deceleration periods at various diluent concentrations are shown in Table 1. These data show that the reaction becomes slower and its maximum rate occurs at early irradiation periods with decreasing TEGDMA content. Bis-GMA exhibits a higher T_g(–7.7°C) than the diluent TEGDMA ($T_g = -81.7$°C), which is generally explained by the presence of strong hydrogen bonding in the former. Hence, this quasi-network hydrogen bonded structure, highly viscous, induced a low radical termination rate just from the irradiation onset, which must be responsible for the short auto-acceleration period, hence only enabling the EPR observation of an auto-deceleration region in lower dilute matrix polymerization. This vitrification period occurred during the cure induces the formation of an inhomogeneous network morphology [4, 12].

The heterogeneity of the curing reaction is enhanced with increasing concentration of bulky, rigid Bis-GMA monomer in the reacting mixture (lower degree of conversion and cross-linking are then expected to be reached) [13].

3.2 Filler concentration effect

Figure 6 shows the variation of free radical concentration ($[R^\bullet]$) with irradiation time (t) up to 300 s, obtained for Bis-GMA/TEGDMA (75/25, wt%) and for this resin with different filler content (0, 10, 20, 30 and 40 wt%). Figure 6 also shows the curves generated using three parameter sigmoidal functions (Eq. 1). Just as in Fig. 5, two different trends (a and b) are observed in Fig. 6: (a) The concentration of free radicals is higher for higher filler loaded matrices over the first irradiation period ($\approx$0−5 s) and (b) At longer irradiation periods ($\approx$5−300 s) an opposite behavior was observed. As for the dilution effect previously described (Fig. 5), the different trends of radical concentration growth correspond to two regimes (a) and (b) (Fig. 6) that are assigned here to stages I–II and III–IV, respectively [5]. This evidence may be explained by an important viscosity influence (higher for higher filler loaded systems) being dominant over the first irradiation stage with filler particles most probably being a constraint to radical termination. Following stages I and II of gelation and during stages III (gelation with reaction diffusion-controlled termination) and IV (vitrification), mainly segmental diffusion and macromolecular conformation changes become possible [5]; consequently, under regime (b) the initial viscosity appears not to affect significantly the kinetics of termination. Even with the filler constraint on radical termination, for the same sample volume, the final radical concentration decreases with filler content (Fig. 6a and Table 2). Because filler loaded resins contained a lower concentration of methacrylate groups/photo-initiator ratio and consequently have generated fewer radicals, it was necessary to correct the radical concentration using the relative concentration of CQ as the correction factor, which was obtained for each composite using CQ concentration in unloaded resin as the maximum value (1 mol%), in order to obtain the effective filler effect on the final radical concentration. The radical concentration represented in Fig. 6a was calculated per total volume

Table 2 Parameters of the sigmoidal (logistic) function (Eq. 1) used to fit the variation of radical concentration with irradiation time for resins with different filler content (FC): correlation factor (χ^2, final reached radical content $[R^\bullet]_f$, time t_h to reach $[R^\bullet]_f/2$ and the empirical constant p

FC (wt%)	0	10	20	30	40
χ^2	0.998	0.998	0.997	0.997	0.995
$[R^\bullet]_f$	307.20 ± 10.74	291.66 ± 9.34	268.99 ± 9.96	245.12 ± 9.85	223.31 ± 12.32
t_h	52.70 ± 4.40	53.79 ± 4.09	54.80 ± 4.71	54.61 ± 4.64	71.24 ± 7.84
p	1.47 ± 0.07	1.27 ± 0.06	1.25 ± 0.08	1.7 ± 0.09	0.91 ± 0.11
$t_{\max}$ (s)	15.20	10.16	9.97	5.08	–[a]

The time $t_{\max}$ to reach the maximum reaction rate is also indicated

[a] Not detectable in the EPR time scale

(see Experimental section); Fig. 6b shows the corrected experimental data. These results indicate that the increase of the final radical methacrylate concentration with filler content may be associated to a reduced radical termination. This radical termination decrease most probably was due to a decrease of the bimolecular reaction and oxygen inhibitor effect promoted by the viscosity rise.

Different monomer reactivity, during gelation (stages I–III) and vitrification (stage IV) periods, is clearly observed in Fig. 6c, where the polymerization rate ($[R^\bullet]'$) is presented as a function of irradiation time, at various filler concentrations. The inflection points ($t_{\max}$) between auto-acceleration and auto-deceleration at various filler concentration are indicated in Table 2. The experimental results presented in Fig. 6c and Table 2 clearly show that: (a) the polymerization mechanism appears to be similar to others reported on the literature for dimethacrylate systems [4, 5, 12]; (b) as expected, all systems point to the presence of a diffusion-controlled kinetics and to gelation occurring at an early reaction stage; (c) the auto-acceleration began earlier and was more pronounced for systems with a higher filler content; (d) the rate of the radical production decreased dramatically after propagation became diffusion controlled and the reaction was subsequently slowed down by vitrification and (e) gelation stage was not observed at 40 wt% filler concentration due to the high viscosity promoted by the presence of high filler loading.

Figure 6c and Table 2 show that systems with lower filler content had a higher reaction rate. The observed kinetics-filler content dependence was attributed to the reduced mobility of pendant double bonds of the lower cross-linked matrix at higher loaded systems. However, we must emphasize that the reactivity of the systems depends on methacrylate group/photo-initiator concentration, which is lower for higher loaded systems, as it was already pointed out.

The depth of cure effect was not taken into account because light propagated through composite samples is only 2 mm thick; hence, it can be assumed that the generated radicals were uniformly distributed.

3.3 Irradiation protocol effect

In order to evaluate the influence of continuously versus interrupted illumination of the monomers, while keeping constant the total curing period, two samples of Bis-GMA/TEGDMA (75/25% by weight) were irradiated over different cumulative periods: (a) 4, 10, 15, 20, 30, 60, 100, 140, 200, 300 s and (b) 60, 180, 300 s. EPR spectra (not shown) were acquired prior to light irradiation and after 60, 180 and 300 s cumulative irradiation periods. More intense signals were obtained when following protocol (b) and, particularly, it was observed an intensity increase of 25% at the end of the irradiation period. These results clearly demonstrate that the polymerization protocol affects the concentration of the radicals generated during the monomer curing.

Most probably, illumination interruptions have contributed to reduce the cross-linking density and DC while favoring molecular oxygen diffusion; consequently, the observed decrease of the final number of radicals when using protocol (a) may be explained by an increase of the yield of the radical termination reaction in the polymerized matrix.

This explanation is consistent with previous studies [14].

3.4 Storage time effect on curing of unfilled and composite resins

In order to study the storage time effect on polymerization of unfilled and loaded resins with 20 wt% filler, EPR spectra were acquired as following: (a) immediately after the sample preparation (described in the Experimental section) and (b) after storing the sample over 10 days at 0°C in the dark. Figure 7 shows the radical concentration variation with irradiation time (0−300 s) for the resin and composite resin under the experimental conditions (a and b). After 10 day storage, it was clearly observed for both systems a reduction of radical concentration just from the initial until the end of the cumulative irradiation periods; this effect was higher for the unfilled resin. Since all the other experimental

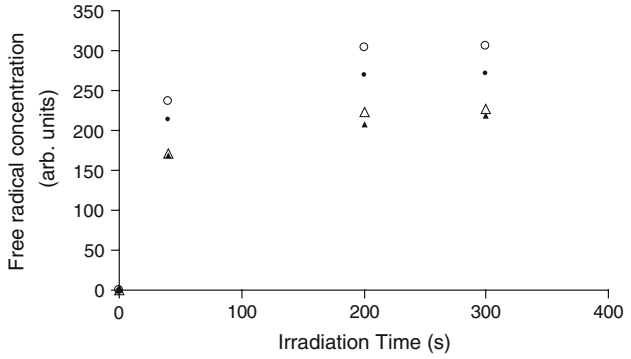

Fig. 7 Free radical concentration variation with irradiation time (0–300 s) for unfilled (○, Δ) and 20 wt% filler loaded (•, ▲) Bis-GMA/TEGDMA (75/25) matrices obtained either immediately (○, •) or 10 days after the sample preparation (Δ, ▲)

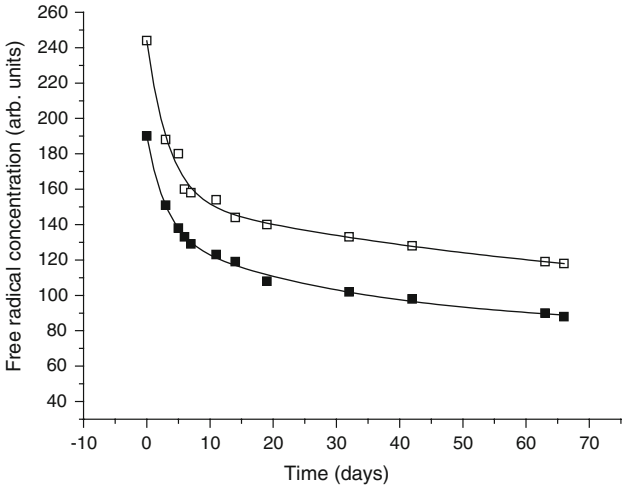

Fig. 8 Free radical decays obtained for Bis-GMA/TEGDMA (75/25) matrices: (□) 0 wt % filler and (■) 30 wt% filler. The curves obtained from exponential fits to the experimental data are also shown

conditions were kept constant, the results suggest that the onset of the reaction took place before the irradiation period, i.e. during the storage period and, consequently, the photopolymerization yield was affected.

As described in the beginning of this section, during the first reaction step, a low viscosity favors the termination process and, consequently, the radical concentration tends to remain low. However, the fact that free radicals were not detected by EPR before irradiation, does not completely rule out the possibility of step I occurrence during sample preparation, in which case either the generated radicals remained below the EPR detection level or would react in both studied systems (a and b). This tentatively explains the observed free radical concentration decreases with storage time. Most probably, this effect is less pronounced in the composite due to restricted mobility of the matrix in the presence of the filler particles [8, 15].

3.5 Aging effect on cured unfilled and composite resins

Preliminary information of the filler loading effect on the concentration decay with time of the generated radicals was obtained in order to evaluate life-time and conformation changes of radicals in cured matrices. For this purpose, the concentration of free radicals in two Bis-GMA/TEGDMA matrices (either unloaded or with a particulate filler) was monitorized over 65 days. EPR peak intensities for both cured systems decreased, but with different rates during sample aging (samples were not kept in the dark). Second order exponential decay functions (3) and (4) were needed to fit the experimental data obtained for 0 and 30 wt% filler loaded resins, respectively (Fig. 8):

$$y = (89.5 \pm 12.5)^{*} \exp[-x/(3.5 \pm 0.7)] + (62.1 \pm 9.2)^{*} \exp[-x/(75.1 \pm 0.7)] + (92.2 \pm 27.4) \quad (3)$$

$$y = (55.1 \pm 6.4)^{*} \exp[-x/(3.0 \pm 0.5)] + (53.1 \pm 3.7)^{*} \exp[-x/(32.8 \pm 11.5)] + (81.9 \pm 6.0) \quad (4)$$

For each resin, the use of double exponential functions with different decay rates (time constants of about 3 days and, at least, 1 month, respectively) reflect the presence of fast and slow processes, respectively. The life-time of radicals (time to reach half of the initial concentration) were 63 and 47 days in the unfilled resin and composite, respectively. These results are consistent with different radical environments and, hence, with different radical reactivity. For free radicals residing in the cured region, it is reasonable to expect that the reactive unpaired electrons remain shielded by the densely cross-linked network and therefore present long life-time decays. The radical decay in cross-linked polymer networks has been investigated before and it has been found that the decay rate of trapped radicals mainly depends on cross-linking density, storage temperature and atmosphere [16]. The present data also show that the half-life of radicals is influenced by the filler; this issue is explained because the stability of the radicals is reduced due to a lower cross-linked degree being reached and to the catalytic effect of glass particle surface [6]. For example, the presence of a catalytic effect of an inorganic filler was previously reported on the curing study of an acrylate mixture and two composites (containing also alumina or hydroxyapatite), which showed lower activation energy [17]. Thus, electrons from base-sites at filler surface may participate in decomposition of radicals. This effect is known to decrease when the filler is treated with a silane coupling agent, like in the present study [17].

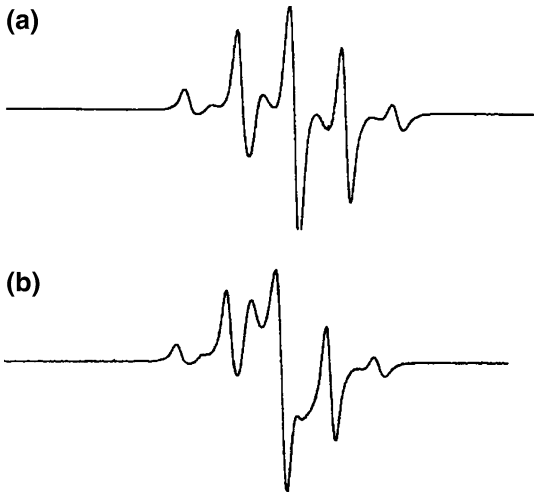

Fig. 9 EPR spectra of Bis-GMA/TEGDMA (75/25) resin obtained: (**a**) immediately after the irradiation period (300 s) and (**b**) after storing the resin for 12 months in the EPR tube at room temperature (about 22°C)

Moreover, it was observed that the lineshape of EPR signal changed with time (Fig. 9). This result suggests that the distribution of CH_2 conformations that contribute to the spectrum also changes with time, implying that the life-time of the radicals depends on its conformation.

The radicals may decay by bimolecular dismutation, where one radical transfers one hydrogen atom to the other or by direct oxidation by O_2 (Fig. 3). The first process is dependent on the distance between radicals, and the latter on the diffusion of oxygen through the polymer. In either case there is a radical that is oxidized by elimination of a hydrogen atom. This mechanism is greatly enhanced in conformations where the abstracted hydrogen atom lies in the same plane as the single-occupied p-orbital containing the unpaired electron (Fig. 4a). However, in the most stable conformation of the radical (Fig. 4b), the C–H bond of the hydrogen atom makes a dihedral angle of 60° with the single-occupied p-orbital, resulting in slower reaction rates. This mechanism should be therefore responsible for the faster depletion of radicals in the conformation A (Fig. 4), as compared to B (Fig. 4) and to the radicals in other possible conformations.

4 Conclusions

Using EPR, it was possible to study the polymerization kinetics through the free radical concentration monitoring during the irradiation period.

The kinetic parameters predicted by the model agree well with the experimental data obtained on dilution and filler content effect studies. At least two regimes were observed during polymerization, which were assigned to previously reported stages (non-diffusion limited, auto-acceleration, reaction-diffusion without propagation limitation and auto-deceleration). It was shown here that photopolymerization of either unfilled or filler loaded dimethacrylate dental materials leads to the presence of long-living free radicals, which remain trapped because of matrix vitrification. Dilution and filler content effects also show two different behaviours over the irradiation period due to discrepancies of viscosity influence on the four polymerization stages. It was found that filler content induces the increase of final radical methacrylate concentration, when both the monomer and the filler components were taken into account to calculate the corrected initiator concentration. Comparatively to unfilled resins, a short free radical life-time was found for the composites, which may be due to the filler surface catalytic effect. Preliminary studies showed that illumination interruptions during the irradiation period promoted a 25% decrease on the final radical concentration, which was also reduced when the starting reaction mixture was stored over 10 days prior to the curing period. The observed changes on the EPR signal lineshape during the post-curing period suggest that the distribution of CH_2 conformations that contribute to the spectrum also changes with time.

Aiming to improve the control of free radical kinetics and life-times, work is now in progress in order to study the influence of plasticizers in composite resin formulations.

Acknowledgements This work has been carried out with financial support of FCT/FEDER (PDCT/SAU-BMA/55935/2004, SFRH/BPD/25112/2005). The authors wish to thank KERR (USA) for kindly providing the filler.

References

1. N. Atherton, H. Melville, D. Whiffen, J. Polym. Sci. **34**, 199–207 (1959)
2. D. Truffier-Boutry, X. Gallez, S. Demoustier-Champagne, J. Devaux, M. Mestdagh, B. Champagne, G. Leloup, J. Polym. Sci. A **41**, 1691–1699 (2003)
3. J. Crivello, K. Dietliker, G. Bradley (ed.), in *Photoinitiators of Free Radical Cationic and Anionic Photopolymerization*, vol III (Wiley, New York, 2002)
4. S.G. Pereira, N. Reis, T. Nunes, Polymer **46**, 8034–8044 (2005)
5. M. Goodner, H. Lee, C. Bowman, Ind. Eng. Res. **36**, 1247 (1997)
6. P. Burtscher, Dent. Mater. **9**, 218–221 (1993)
7. F. Bauer, H. Ernst, D. Hirsch, S. Naumov, M. Pelzing, V. Sauerland, R. Mehnert, Macromol. Chem. Phys. **205**, 1587–1593 (2004)
8. T. Nunes, S.G. Pereira, S. Kalachandra, J. Mater. Sci. Mater. Med. **19**, 1881–1889 (2008)
9. L.G. Lovell, K.A. Berchtold, J.E. Elliott, H. Lu, C.N. Bowman, Polym. Adv. Technol. **12**, 335–345 (2001)
10. A. Ferretti, G. Costante, A. Ponti, Res. Chem. Int. **28**, 159–174 (2002)
11. D. Sustercic, N. Funduk, M. Pintar, J. Mater. Sci. Mater. Med. **8**, 507–515 (1997)

12. I. Sideridou, V. Tserki, G. Papanastasiou, Biomaterials **23**, 1819–1829 (2002)
13. S.G. Pereira, T. Nunes, S. Kalachandra, Biomaterials **23**, 3799–3806 (2002)
14. F. Gonçalves, F. Calheiros, M.F. Witzel, Y. Kawano, R. Braga, J. Biomed. Mat. Res. Part B Biomat. **82b**, 89–92 (2007)
15. S.G. Pereira, R. Osorio, M. Toledano, M.A. Cabrerizo-Vilchez, T.G. Nunes, S. Kalachandra, Dent. Mater. **23**(10), 1189–1198 (2007)
16. J. Lapcik, J. Jancar, A. Stasko, P. Saha, Mater. Sci. Mater. Med. **9**, 257–262 (1998)
17. T.M. Chu, J. Halloran, J. Am. Ceram. Soc. **83**, 2375–2380 (2000)